Open access • Journal Article • DOI:10.1080/13632460701457116

Site classification using horizontal-to-vertical response spectral ratios and its impact when deriving empirical ground-motion prediction equations

Yoshimitsu Fukushima, Luis Fabian Bonilla, Oona Scotti, John Douglas

Institutions: Shimizu Corporation, Institut de radioprotection et de sûreté nucléaire

Published on: 14 Aug 2007 - Journal of Earthquake Engineering (Taylor & Francis Group)

Site Classification Using Horizontal-to-vertical Response Spectral Ratios and its Impact when Deriving Empirical Ground-motion Prediction Equations

Yoshimitsu Fukushima, L.F. Bonilla, Oona Scotti, John Douglas

Site classification using horizontal-to-vertical response spectral ratios and its impact when deriving empirical ground-motion prediction equations

Yoshimitsu Fukushima[(1)], Luis Fabián Bonilla[(2)], Oona Scotti[(2)], and John Douglas[(3)]

(1) Shimizu Corporation, Tokyo, Japan

(2) Institut de Radioprotection et de Sûreté Nucléaire, Fontenay-aux-Roses, France

(3) BRGM, Orléans, France

Abstract

We classify sites based on their predominant period computed using average horizontal-to-vertical (H/V) response spectral ratios and examine the impact of this classification scheme on empirical ground-motion models. One advantage of this classification is that deep geological profiles and high shear-wave velocities are mapped to the resonance frequency of the site. We apply this classification scheme to the database of Fukushima et al. (2003), for which stations were originally classified as simply rock or soil. The calculation of average H/V response spectral ratios permits the majority of sites in the database to be

unambiguously classified. Soft soil conditions are clearly apparent using this technique. Ground-motion prediction equations are then computed using this alternative classification scheme. The aleatoric variability of these equations (measured by their standard deviations) is slightly lower than those derived using only soil and rock classes. However, perhaps more importantly, predicted response spectra are radically different to those predicted using the soil/rock classification. In addition, since the H/V response spectral ratios were used to classify stations the predicted spectra for different sites show clear separation. Thus, site classification using the predominant period appears to be partially mapped into the site coefficients of the ground-motion model.

Keywords: H/V / response spectral ratio / site classification / attenuation relation / predominant period

1. Introduction

It is well known that precise site classification is important in determining accurate empirical ground-motion prediction relations. However, possessing a good knowledge of site conditions is rather exceptional. Even well

characterized sites do not always have complete geotechnical information down to the bedrock. For example in Japan, the surface array K-net has geotechnical characterization down to a maximum depth of 20 m. Thankfully, its complementary borehole array KiK-net, has information down to 100 or 200 m depth depending on the site (Pousse et al., 2005). This important, but expensive, information is almost non-existent for most strong-motion networks in the world, and Europe is not an exception. Some previous European empirical ground motion prediction relations (e.g. Berge-Thierry et al., 2003; Fukushima et al., 2003) used a general rock/soil classification scheme due to this lack of detailed site information. This site classification, based mainly on geological information, came with the strong-motion data provided by the data contributing agencies. A general soil class, however, may contain both stiff and soft soils, and a general rock class may include sites with weathered rock or thin soil layers at the surface and hard bedrock stations. In addition, the difference between predicted ground motions at soil and rock stations predicted by these relations is not remarkable, being less than 70% (Fukushima et al., 2003). Therefore, a better site classification is required for precise strong ground motion estimation.

Site classification is ultimately related to site amplification effects. These can vary from simple 1D to complex 3D effects depending on the geometry and impedance contrast of the ground structure. Such effects can only be calculated for a few specific locations, for example the Los Angeles basin and Ashigara valleys, where 3D ground structural information has been acquired (e.g. Olsen and Archuleta, 1996; Pitarka et al., 1994). Nonetheless, even at these locations, the maximum frequency of the computed basin response is about 1 Hz, being proportional to the degree of knowledge of the geological structure for wavelengths of a few hundred meters.

In particular situations, an approximation of the theoretical site amplification can be computed using 1D multiple reflection theory. Yet, the cost of deep boring, down to the bedrock, at all sites is unrealistic. In the USA, average shear-wave velocity in the first 30 m, here after called Vs30, is used as an alternative parameter to classify soil conditions (Table 1). This parameter provides more information than surface geological data since impedance contrast at least down to this depth is reflected in the site classification. However, the transfer function should not be limited to the first 30m; on the contrary, it should be continued down to bedrock.

An alternative, but less well-known, site classification scheme originally proposed by Kanai and Tanaka (1961) is based on the site's predominant period. This is used in Japan for the seismic design code of highway bridges (Japan Road Association 1980, 1990), and it is also given in Table 1. This classification does not exactly correspond to the Vs30 scheme, but it represents a combination between Vs and the thickness of soil layers. One advantage of this classification is that deep geological profiles and high shear-wave velocities are mapped to the resonance frequency. A recent study using Japan data (Zhao et al., 2006) proposed four site categories using this method. These authors used this site classification rather than the traditional description based on Vs30 because thick stiff soil layers overlying hard rock amplify long-period motions. Conversely, thin soft soil layers amplify short periods. This means that Vs30 does not always capture the predominant period of the site, since it represents only the shallowest portion of the geological profile. A similar technique was successfully applied by Lang and Schwarz (2006) for sites in California. Using a classification scheme based on predominant period presents two advantages. The first one is that strong-motion prediction will account for the entire site frequency content and not only shallow geological effects. In addition, at many

sites easily available direct field measurements can be performed to estimate the site predominant period using either ambient noise measurements or H/V spectral ratios on earthquake data (e.g. Bonnefoy-Claudet et al., 2006). Furthermore, when computing empirical ground-motion prediction relations, Lussou et al. (2001) showed that, for K-net data, site classification by a combination of Vs30 and H/V predominant period reduced the standard deviation of the computed equation. Zhao et al. (2006) classified K-net sites using average H/V response spectral ratios and obtained a relation that well modeled local site effects and also reduced the model's uncertainty. This procedure potentially has application to data classified into general categories such as rock or soil, or that use no classification at all.

In the present study, we use the H/V response spectral ratio, which was proposed by Zhao et al. (2006), to attempt a site classification based on predominant period. It is not the objective of this paper to derive new empirical ground-motion estimation equations. We rather focus on the site classification procedure, its shortcomings and its general impact on the shape of the predicted response spectra.

2. Data

In this paper, we use the data used by Fukushima et al. (2003) to derive empirical ground-motion prediction equations. This dataset mainly consists of recorded strong motion from west Eurasia (mainly Europe). However, to better constrain near-fault saturation parameters, earthquakes from California and the 1995 Hyogo-ken Nanbu (Kobe) (Japan) earthquakes were included. Only shallow crustal earthquakes are selected in order to derive models for a homogeneous tectonic environment. We also adopt the same magnitude scale and distance metric as Fukushima et al. (2003). Namely, magnitude *M* is the moment magnitude *Mw* when available; otherwise *Ms* (the surface-wave magnitude) is used (this is used for a number of smaller European events). The distance is defined as the closest distance from the site to the rupture for the Kobe and Kocaeli earthquakes (taken from Fukushima et al., 2000; 2002), otherwise it corresponds to hypocentral distance. Two stations were eliminated from the original database because they were suspected of having soil-structure interaction (Yonago and Ohsaka of BRI from the Kobe data). The number of events considered in this study is 50 recorded at 341 strong-motion stations.

The data ranges are, for distance, 0.5 to 235 km and, for magnitude, 5.5 and 7.4 (Figure 1).

3. Site classification

Zhao et al. (2006) classified their sites according to the predominant period computed using the H/V response spectral ratio. They used the 5% damping response spectra ratio between the horizontal and vertical components as an approximation for smoothed Fourier spectral ratios. Their reasoning was that the response spectra are closer to engineering needs than Fourier spectra. Moreover, individual site H/V amplitudes are not important, but the predominant period is. In this way, they proposed four site categories for Japan (Figure 2, top). Figure 2 (bottom) shows the standard deviation of their average H/V response spectral ratios. Note that all site classes have a standard deviation value close to 0.4, representing a variability of 50%.

Following the same procedure in this article, only records having three components (two horizontal and one vertical) were used to compute the H/V response spectral ratio. In the present study, average H/V response spectral

ratios were used to classify stations, and in this regard, the two horizontal components were considered individually. Mean residuals between observed and predicted response spectra from the equations of Fukushima et al. (2003) were subsequently inspected, since analysis of residuals proved to be useful when the observed response spectra showed amplification with respect to the predicted accelerations. A first attempt was made to classify the sites according to the Japanese soil classification. Figure 3 shows an example of H/V response spectral ratios (top) and residuals (bottom) (for the Messina station in Italy). The Japanese H/V response spectral ratios from Zhao et al. (2006) are also plotted. This station is actually classified as a rock site in the original database of Fukushima et al. (2003). However, a peak around 0.3s is observed on the H/V plot as well as a remarkable amplification in the residuals near 0.4s. This station could then be classified as SC-II according to the Japanese spectral shapes.

Classification is, however, not always straightforward. The observed H/V response spectral ratio may not present a peak, but rather a broadband behavior as shown in Figure 4 for the San Francisco Airport station. This site is located on soft ground (McGarr et al., 1991), therefore, complex soil amplification could be expected, such as through nonlinear behavior, and the

current site classification does not account for such soil behavior making this station impossible to classify. For stations that recorded the Kobe earthquake in Japan, the first author had *a priori* geotechnical information. However, in order to have a homogeneous procedure, all stations were classified as if only the H/V information was known. Since few (roughly 30%) stations have multiple records the average H/V response spectral ratio per site is not statistically robust. Therefore, automatic classification as proposed by Zhao et al. (2006), based on a probabilistic distribution of the spectral shape, cannot be used. Thus in this study, all sites were manually classified.

During the classification procedure, each co-author independently provided their opinion. It became apparent that the frequency band for soil class SC-III is too narrow, and for all purposes inapplicable. Therefore, we decided to combine SC-II and SC-III into a single class for our study. The final site categories are SC-1 (SC-I), SC-2 (SC-II plus SC-III), and SC-3 (SC-IV), respectively. Finally, those sites that could not be classified maintained their original denomination of rock (SC-4) and soil (SC-5), respectively (Table 2). These last two classes, however, are only retained so as to have enough data to compute ground-motion prediction equations.

Once the definitions of the site classes were finalized, each co-author manually classified each station. For roughly 90% of the stations, the classifications agreed with each other. Different classifications were made for stations close to the limits of the site classes. When opinions differed, stations were re-classified after further discussion. Final statistics of the classification are summarized in Table 3, which shows the number of stations that switched from original rock and soil categories to the new classes based on predominant period. Note that sites originally classified as rock were reclassified into all three new categories, SC-2 being the more common. Similarly, the original soil category was composed of a combination of all three new types of sites; in this case, SC-2 and SC-3 classes most represented. Note that we were able to classify 47 sites out of 91 rock sites and 171 sites out of 250 soil sites using the procedure (64% in total).

Following Zhao et al. (2006), we computed the mean H/V response spectral ratio and its standard deviation for each site class (Figure 5). Note the remarkable similarity between the Japanese H/V averages and those derived here. It should be noted that less than 4% of Japanese stations belong to soil class SC-III (Zhao et al., 2006) suggesting that class SC-2 closely corresponds

to class SC-II in Japan because, as noted above, SC-III was found to be too narrow, here, to use for classification of stations (i.e. very few stations fell within this category). With respect to the standard deviations, the ones computed in this study show less variation with respect to period than those of Zhao et al. (2006); however, their absolute levels are similar. This is rather surprising considering the fewer records used in this study compared to those used by Zhao et al. (2006).

Statistics of individual classes and regions are indicated in Table 4 for all 341 sites. Many SC-1 and SC-2 stations are located in west Eurasia, whereas SC-3 stations are equally represented in the three regions.

4. Regression analysis

In this study, the same functional form as Fukushima et al. (2003) is used, namely:

$$\log_{10}(Sa(f)) = a(f)M - \log_{10}(R + d(f)*10^{e(f)M}) + b(f)R + \Sigma c_j\,(f)\delta_j \qquad (1)$$

where *Sa(f)* is the elastic response spectral acceleration for 5% damping. *M* is magnitude, *R* is hypocentral distance or shortest distance to the rupture (for the Kocaeli and Kobe earthquakes) and *a*, *b*, c_j and *d*, are frequency-dependent regression coefficients. The suffix *j* corresponds either to the general rock/soil classes (reference computation) or to the proposed 5 site classes (predominant period classification). The variable δ_j is a dummy variable, which is equal to 1 if data are observed at *j-th* site category and 0 otherwise. The coefficient *e(f)* is fixed as 0.42 to ensure the stability of the regression procedure. A magnitude-distance filter is applied in order to avoid distant records from small events biasing the results. For the calculation of the empirical ground-motion equations, we use both horizontal records, which are considered to be independent. The interested reader is referred to Fukushima et al. (2003) for details.

5. Results and Conclusions

Recall that we do not seek to derive a new ground-motion model for use in seismic hazard assessment. Therefore, we limit ourselves to commenting on the effect of the new site classification on: the derived site coefficients, the

standard deviations of the model, and predicted response spectra. Data were band-pass filtered with cut-offs of 0.25 and 25Hz (Fukushima et al., 2003). Thus, all results are shown up to 3 s in order to avoid possible bias due to filter effects (e.g. Boore and Bommer, 2005).

Site Coefficients

Figure 6 shows the relative amplification of site classes SC-1, SC-2, and SC-3 with respect to the general rock site classification SC-4. The SC-1/rock ratio is close to unity, except for a slight increase at long periods, which indicates that the general rock class captures the main features of rock/stiff soil behavior. The slight difference at long periods occurs since the general rock category also contains medium to soft soil sites, as mentioned above. Nonetheless, the overall effect of mixing site conditions within a general rock category is rather small. Conversely, the SC-2/rock ratio shows deamplification of 50% at short periods and an amplification of two at long periods. The SC-3/rock ratio demonstrates a slightly greater deamplification than the SC-2/rock results and, in addition, it clearly indicates an amplification factor up to 3.3

around 1s. Note that the general soil/rock ratio does not display deamplification and the maximum amplification is only about 70% at 1s. Another interesting result is the order of PGA amplification using this new classification: PGA at SC-3 sites is less amplified than at SC-2 stations, which, in turn, is less amplified than at sites in the SC-1 class. Unfortunately, this method has limitations since there are sites that do not exhibit clear H/V peaks, on the contrary they show broadband response, which is not captured by any of the classes. Site response at these stations remains difficult to quantify irrespective of the classification scheme.

Standard Deviation

Figure 7 shows a slight reduction (on average 2%) in the standard deviation compared to the original rock/soil classification scheme. This result suggests that better knowledge of local site conditions can reduce aleatoric variability in empirical ground-motion models. Therefore, more effort should go into site characterization in order to derive more accurate strong-motion models with lower uncertainties.

Predicted response spectra

Figure 8 shows that the shape of the predicted response spectra follows the shape of their corresponding average H/V response spectral ratios since these ratios were used in the classification process. This is less evident for SC-3 sites, although the amplification of spectral accelerations at long periods is remarkable. Incidentally, note that the period intervals defining such classes (Table 3) are apparent in the predicted response spectra. This suggests that site classification using predominant periods could be partially mapped into the site coefficients. This provides a useful link between strong ground motion predictions and earthquake-engineering design against soil-structure interaction.

Predicted spectral accelerations at SC-1 sites are slightly higher than those at general rock sites. This is an interesting result considering that SC-1 and the general rock class are similar in terms of site amplification (Figure 6). This shows that the choice of site classification scheme has considerable impact on predicted ground motions. Recall that most SC-1 sites are located in west Eurasia (Table 4), thus these results may be regionally biased. Conversely,

response spectra on sediments show distinct behavior depending on whether the ground is composed of medium or soft material (SC-2 and SC-3 classes). Note that sites of the SC-3 class are almost equally represented in the three geographical regions, thus predicted response spectra may represent the average behavior of such sites and tectonic environments.

Given the quality of these dataset and the lack of quantitative knowledge of the velocity profile at each site, we cannot say which empirical median predictions are more correct. Additional studies should be performed, in Japan for example, to help resolve this practical question. Nonetheless, we can see that this site classification clearly reproduces some seismological observations. For example, predicted PGA for the three site classes are well separated. This separation is also maintained at other periods, from high spectral accelerations at short periods (stiff sediments) to low spectral amplitudes at long periods (soft soils). These results already show an improvement with respect to general rock/soil classes whose predicted spectral accelerations show little difference at short periods, and the PGA at rock sites is lower than at soil sites (Figure 8).

Good knowledge of site conditions is important for deriving accurate empirical ground motion prediction equations. In this study we used a site classification procedure based on the predominant resonance period computed from average H/V response spectral ratios and applied it to the database of Fukushima et al. (2003). The most remarkable result is the similarity of both spectral amplitudes and shapes of average H/V response spectral ratios to those found in Japan using the same technique (Zhao et al., 2006). This suggests that a common site classification scheme may be possible regardless of the geology and geographical location of a given site. However, the physical meaning of such shapes and their correspondence with Vs30 classification still remains to be clarified. We also found that previous general rock/soil categories are, in fact, composed of rock/stiff, medium and soft soils. The relative amplification of these new classes (SC-2 and SC-3) with respect to the general rock category is about 2.0 and reaches a maximum of 3.3 at 1s. On the other hand, SC-1 and general rock classes share similar amplification effects. The standard deviations of the derived ground-motion model using these new site classes are slightly lower than that obtained using general rock/site classes. Despite this small reduction, this result encourages the pursuit of a better site

classification in order to improve the accuracy of empirical models. Predicted response spectra using the new classes have similar spectral shapes to the average H/V response spectral ratios that define each class. This is useful for predicting the period of the maximum spectral acceleration. This, however, represents a shortcoming of the method because sites having a broadband response cannot be accurately classified. In any case, this simple technique allows a fast evaluation of site effects when geotechnical characterization of the site does not exist. In addition, the method can allow the direct incorporation of effects involving deep soil structure and average shear-wave velocity of the whole soil deposit into empirical ground-motion prediction equations.

Our scheme may be useful for site classification even when information on the soil profile is lacking. However, strong-motion data are not always available in low seismicity areas. Alternative classification using the H/V spectral ratios from microtremors (Nakamura, 1989) may be useful in this regard. The practical use of microtremor was first attempted by Kanai and Tanaka (1961) as well as by Lang and Schwartz (20006) recently. However, extending the application of the procedure followed here to microtremors will require more careful investigation of comparisons between strong motion and microtremor,

H/V spectral ratios.

Acknowledgements

We would like to express our gratitude to Dr. J. Zhao from GNS, New Zealand, for his help with this study. We would also like to acknowledge all organizations that provided strong-motion data. This manuscript was improved by thoughtful comments of an anonymous reviewer and Dr. D. Boore.

References

Berge-Thierry, C., D. A. Griot-Pommera, F. Cotton and Y. Fukushima (2003). New empirical response spectral attenuation laws for moderate European earthquakes, *J. Earthq Eng.,* 7(2), 193-222.

Bonnefoy-Claudet, S., C. Cornou, P.-Y. Bard, F. Cotton, P. Moczo, J. Kristek and D. Fäh (2006). H/V ratio: a tool for site effects evaluation. Results from 1-D noise simulations, *Geophys. J. Int.*, 167, 827-837.

Boore, D. M. and J. J. Bommer (2005). Processing of strong-motion accelerograms: needs, options and consequences, *Soil Dyn. & Earthq. Eng.,* 25, 93-115.

Building Seismic Safety Council (2000). The 2000 NEHRP Recommended Provisions for New Buildings and Other Structures: Part I (Provisions) and Part II (Commentary), FEMA 368/369, Federal Emergency Management Agency, Washington, D.C.

Fukushima, Y., K. Irikura, T. Uetake and H. Matsumoto (2000). Characteristics of observed peak amplitude for strong ground motion from the 1995 Hyogo-ken Nanbu (Kobe) earthquake, *Bull. Seism. Soc. Am.*, 90, 545-565.

Fukushima, Y., O. Köse, T. Yürür, P. Volant, E. Cushing, R. Guillande (2002). Attenuation characteristics of peak ground acceleration from fault trace of the 1999 Kocaeli (Turkey) earthquake and comparison of spectral acceleration with seismic design code, *J. Seismology*, 6, 379-396.

Fukushima Y., C. Berge-Thierry, P. Volant, D. A. Griot-Pommera, F. Cotton (2003). Attenuation relation for west Eurasia determined with recent near-fault records from California, Japan and Turkey, *J. Earthq Eng.,* 7(3), 1-26.

Japan Road Association (1980). Specifications for Highway Bridges Part V, Seismic Design, Maruzen Co., LTD.

Japan Road Association (1990). Specifications for Highway Bridges Part V, Seismic Design, Maruzen Co., LTD.

Kanai K. and T. Tanaka (1961). On Microtremors. VIII, *Bull. Earthr. Res. Inst., Tokyo Univ.,* 40, 97-114.

Lang, D.H. and J. Schwarz (2006). Instrumental subsoil classification of Californian strong motion sites based on single-station measurements, Proc. 8th U.S. National Conf. Earthq. Eng., San Francisco, Paper No. 120.

Lussou,P., P.Y. Bard, F. Cotton Y. and Fukushima (2001). Seismic design regulation codes: Contribution of K-net data to site effect evaluation, *J.*

Earthq. Eng., 5, 13-33.

McGarr, A., M. Çelebi, E. Sembera, T. Noce, and C. Mueller (1991**).** Ground motion at the San Francisco international airport from the Loma Prieta earthquake sequence, 1989, *Bull. Seism. Soc. Am.,* 81, 1923-1944.

Nakamura, Y. (1989). A method for dynamic characteristics estimation of subsurface using microtremor on the ground surface, *Quart. Rep. Railways Tech. Res. Inst*. 30**,** 25–33.

Olsen, K. and R.J. Archuleta (1996). Three-dimensional simulation of earthquakes on the Los Angeles fault system, *Bull. Seism. Soc. Am.,* 86, 575-596.

Pitarka, A., H. Takenaka, and D. Suetsugu (1994). Modeling of strong motion in the Ashigara Valley for the 1990 Odawara, Japan, earthquake, *Bull. Seism. Soc. Am.,* 84, 1327-1335.

Pousse, G., C. Berge-Thierry, L.F. Bonilla, and P-Y, Bard (2005). Eurocode 8 design response spectra evaluation using K-net Japanese database, *J. Earthq Eng.,* 9(4), 547-574.

Zhao, J. X., K. Irikura, J. Zhang, Y. Fukushima, P. G. Somerville, A. Asano, Y. Ohno, T. Oouchi, T. Takahashi and H. Ogawa (2006), An Empirical Site-Classification Method for Strong-Motion Stations in Japan Using H/V Response Spectral Ratio, *Bull. Seism. Soc. Am.*, 96, 914-925.

Table 1. Site class definition used in Japan for engineering design practice (Japan Road Association 1980 and 1990) and the approximate correspondence with NEHRP site classes (BSSC, 2000).

Site classes	Site natural period (s)	Average shear-wave velocity	NEHRP class
SC-I	$T_G < 0.2$s	$V_{s30} > 600$ m/s	A+B
SC-II	$0.2\text{s} \le T_G < 0.4$s	$300\text{ m/s} \le V_{s30} < 600$ m/s	C
SC-III	$0.4\text{s} \le T_G < 0.6$s	$200\text{ m/s} \le V_{s30} < 300$ m/s	D
SC-IV	$0.6\text{s} \le T_G$	$V_{s30} < 200$ m/s	E

T_G of K-net station is simply estimated by $T_G = 4H/Vs$, where H is thickness of upper layer than rock or stiff soil in (m), and Vs is average S wave velocity of the layer in (m/s)

Table 2. Site class definition used in this study and the approximate correspondence with NEHRP site classes (BSSC 2000).

Site classes	Site natural period (s)	Average shear wave velocity	NEHRP class
SC-1	$T_G < 0.2$s	$V_{s30} > 600$ m/s	A+B
SC-2	$0.2\text{s} \le T_G < 0.6$s	$200\text{ m/s} \le V_{s30} < 600$ m/s	C+D
SC-3	$0.6\text{s} \le T_G$	$V_{s30} \le 200$ m/s	E
SC-4	Unknown	$V_{s30} > 800$ m/s	A+B
SC-5	Unknown	$300\text{ m/s} \le V_{s30} < 800$ m/s	C

SC-4 and SC-5 are general rock and soil classes that were impossible to classify using the new procedure.

Table 3 Number of sites in each category using the proposed and original classification schemes.

Site classes	SC-1	SC-2	SC-3	SC-4	SC-5	Total
Rock	12	23	12	44		91
Soil	11	77	83		79	250
Total	23	100	95	44	79	341

Table 4. Number of sites per region and site class.

Region	SC-1	SC-2	SC-3	SC-4	SC-5	Total
West Eurasia	20	63	29	34	51	197
Japan	1	10	39	6	6	62
USA	2	27	27	4	22	82
Total	23	100	95	44	79	341

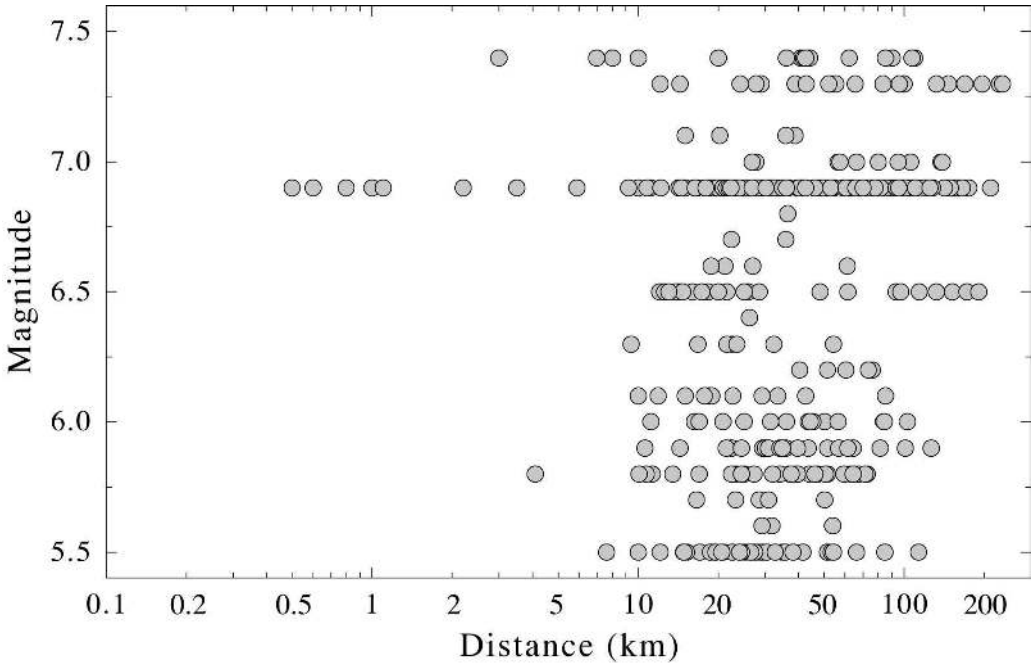

Figure 1. Magnitude-distance distribution of the records used.

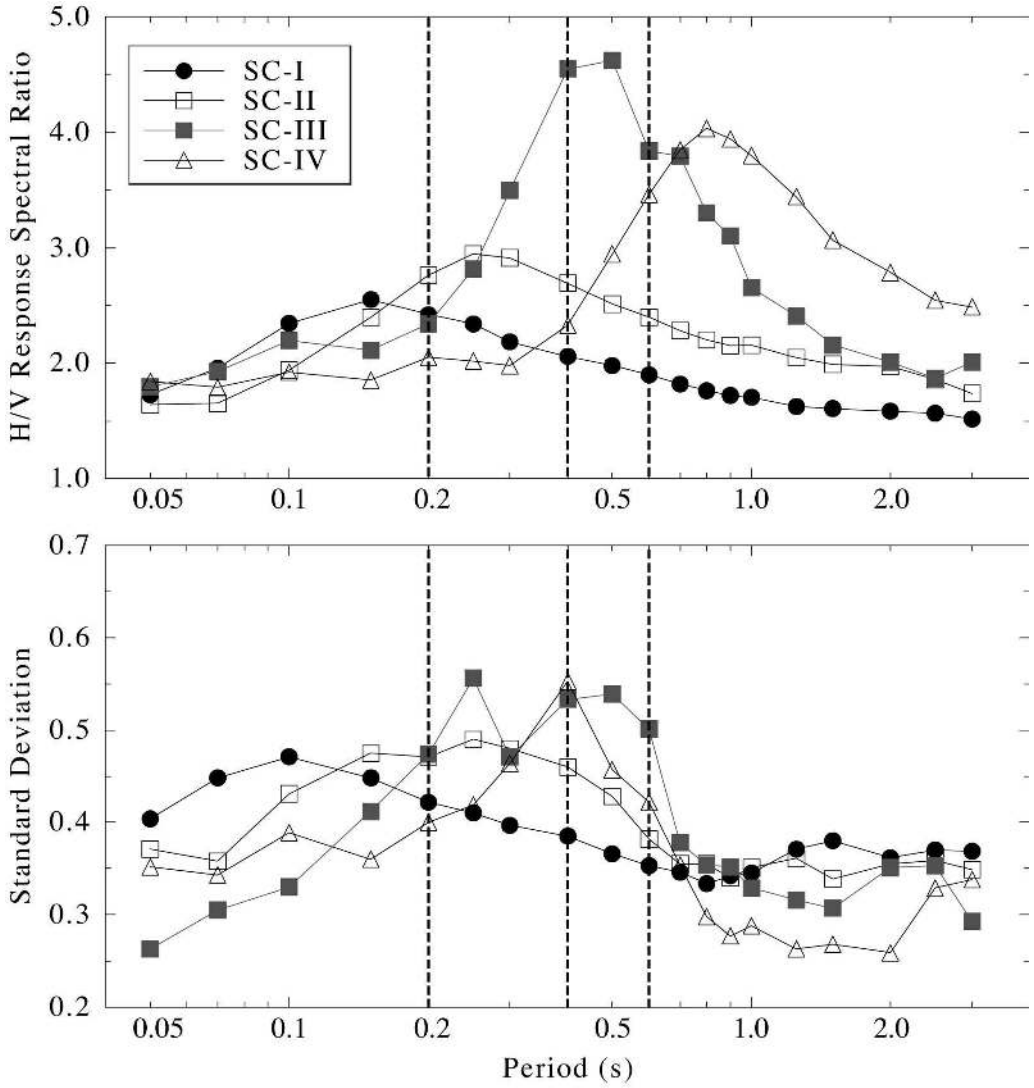

Figure 2. Average H/V response spectral ratio for the Japanese site classes (top) and standard deviation for each class (bottom). The standard deviation is computed using natural logarithms of the ratios. The vertical dashed lines represent the limits of the period intervals for each site class. Results from Zhao et al. (2006).

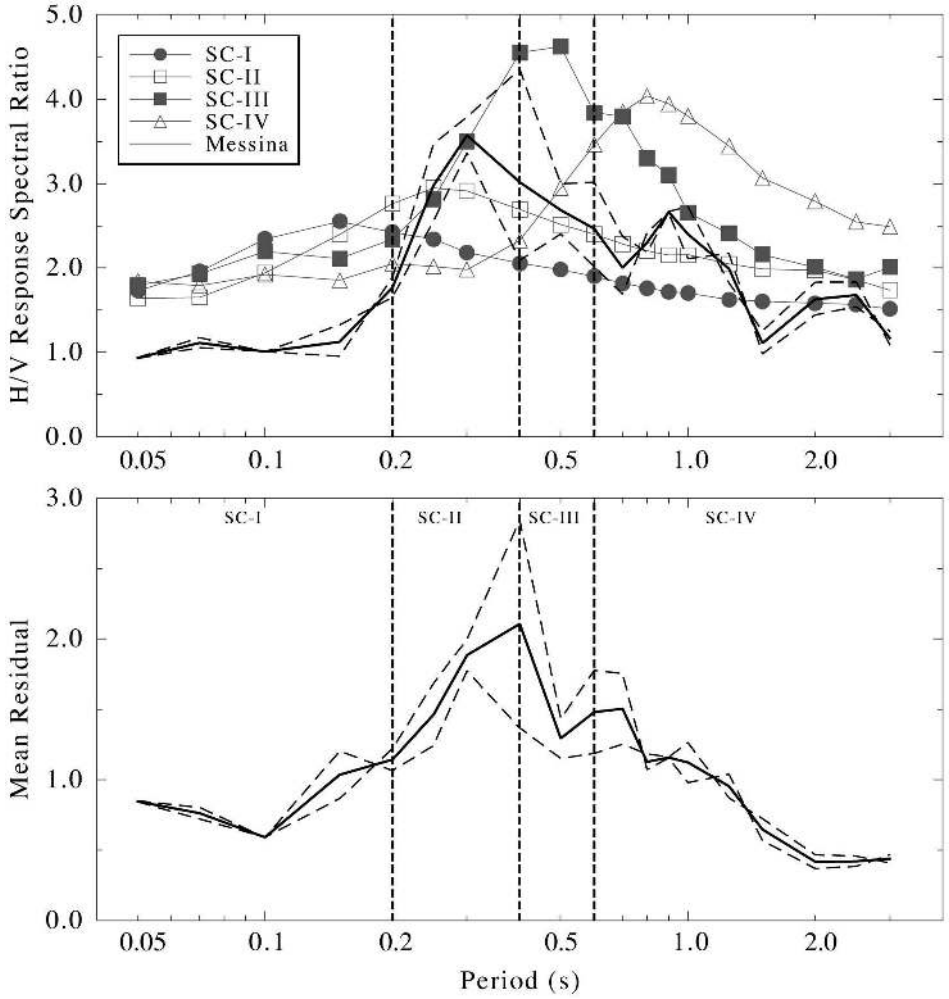

Figure 3. Average H/V response spectral ratios for the Messina station in Italy (top) showing, for comparison, the results for the four Japanese four site classes. Mean residuals between observed and predicted response spectra from the Fukushima et al. (2003) model (bottom). In both plots, estimates for each component are shown. Most stations had only one record contributing two horizontal components, which were assumed to be independent.

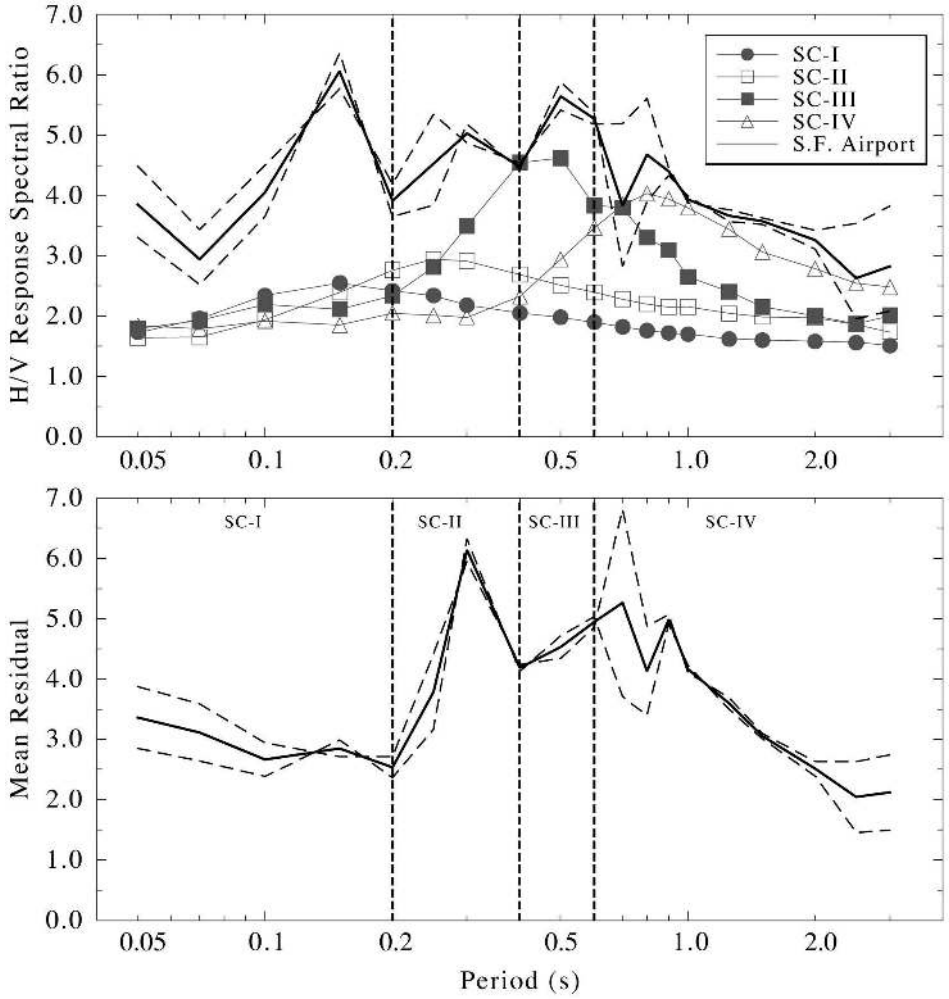

Figure 4. Same as Figure 4, but for station at San Francisco Airport in the USA. Note the broadband site response. This kind of behavior is not taken into account in the Japanese site classification; therefore the site cannot be classified.

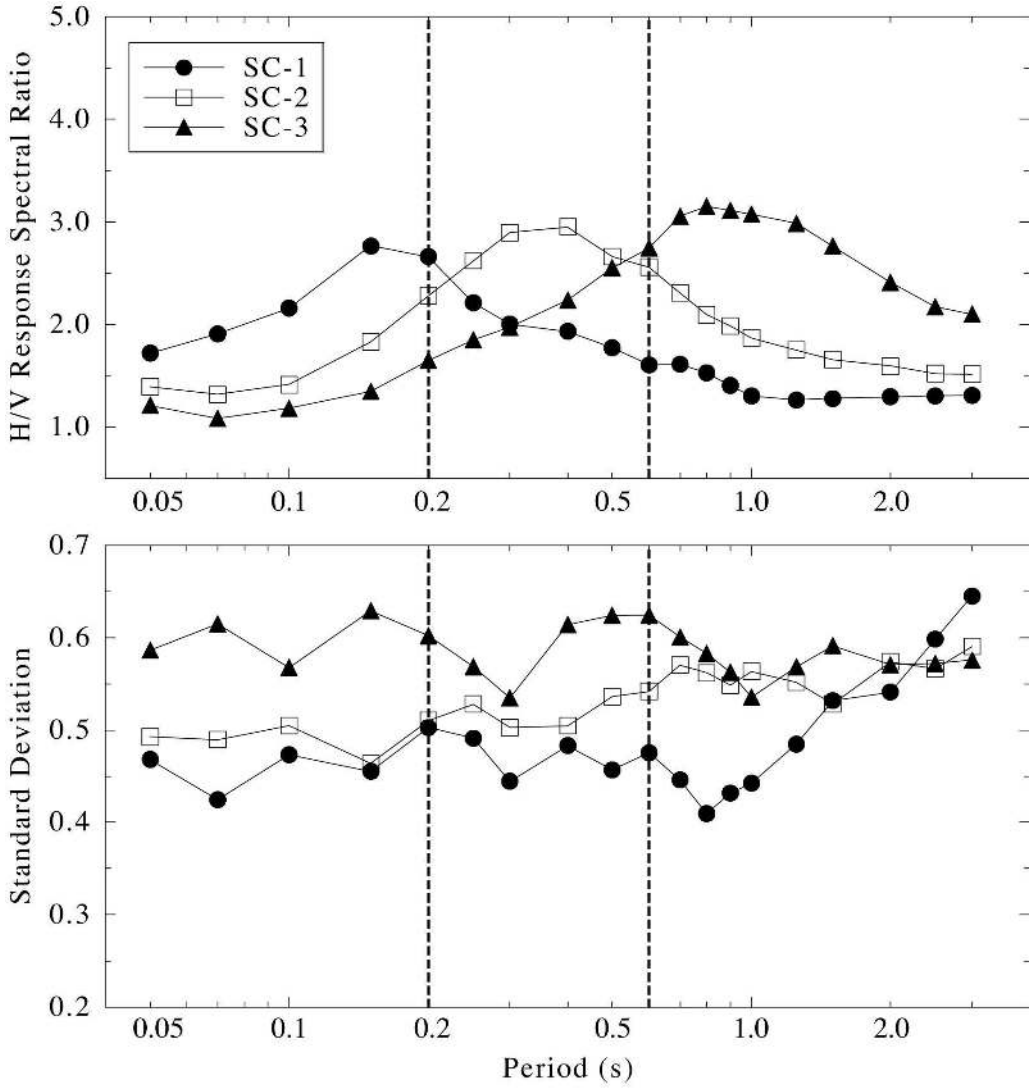

Figure 5. Average H/V response spectral ratios (top) and standard deviations based on spectral ratios in natural logarithms (bottom) for the site classes used in this study.

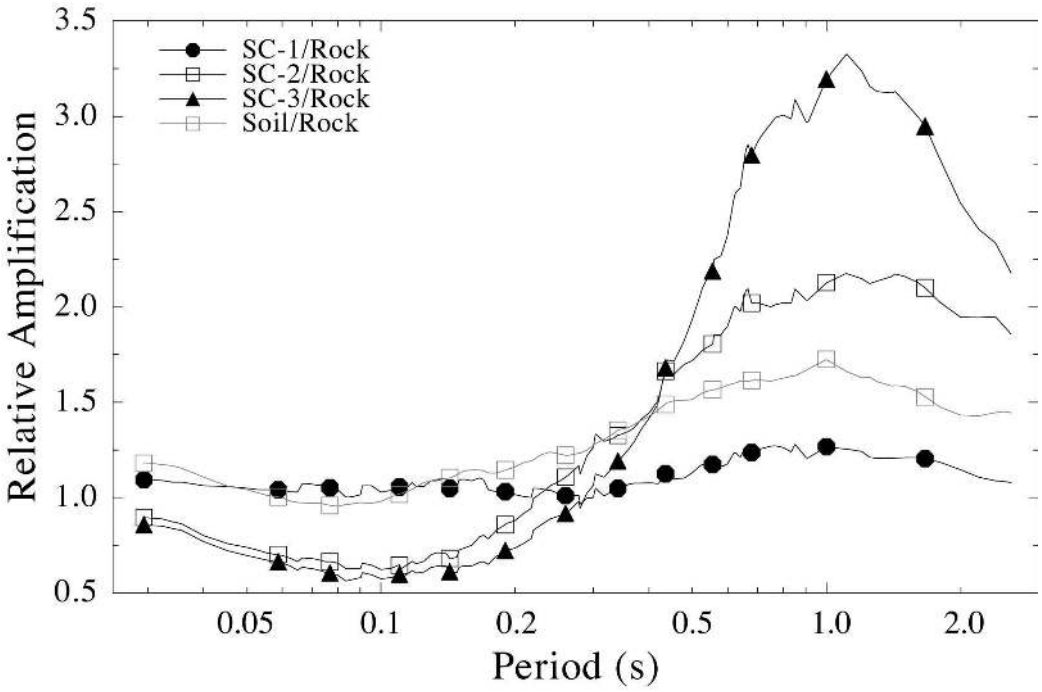

Figure 6. Relative amplification of site classes used in this study, SC-1, SC-2, and SC-3, with respect to general rock site classification. For comparison, general soil-to-rock amplification is also shown. Note that amplification for SC-1 and general rock classes are similar.

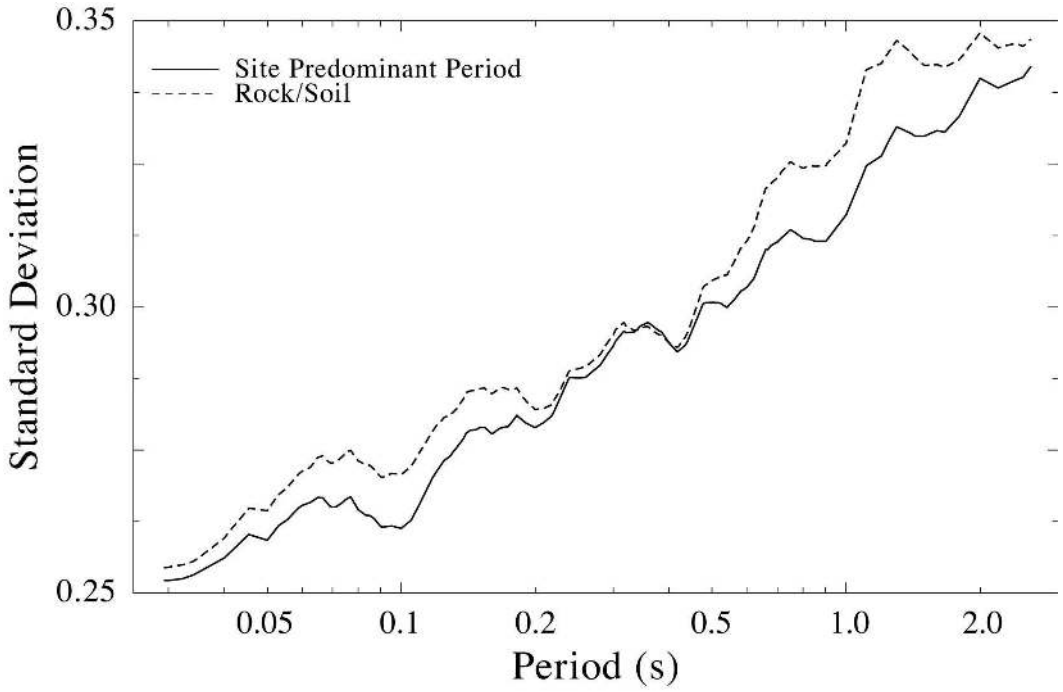

Figure 7. Overall standard deviation obtained using predominant period classification (solid line) and general rock/soil classes (dashed line) in log 10 logarithms. This figure suggests that a better site classification scheme reduces, albeit slightly, the aleatoric variability of the ground-motion model.

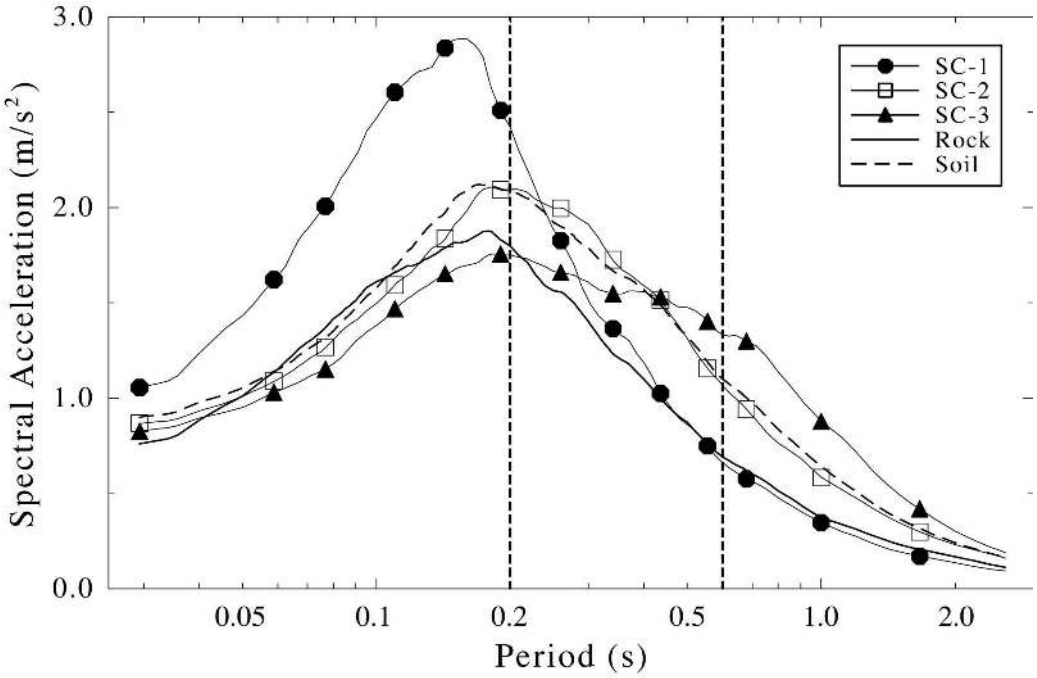

Figure 8. Predicted response spectra for a magnitude 6.0 earthquake at 30 km using the site classes proposed in this study and general rock/soil categories.